High energy efficiency and high power density proton exchange membrane fuel cells — electrode kinetics and mass transport

Supramaniam Srinivasan, Omourtag A. Velev, Arvind Parthasarathy, David J. Manko and **A. John Appleby**

Center for Electrochemical Systems and Hydrogen Research, Texas Engineering Experiment Station, Texas A&M University System, College Station, TX 77843-3402 (U.S.A.)

Abstract

The development of proton exchange membrane (PEM) fuel cell power plants with high energy efficiencies and high power densities is gaining momentum because of the vital need of such high levels of performance for extraterrestrial (space, underwater) and terrestrial (power source for electric vehicles) applications. Since 1987, considerable progress has been made in achieving energy efficiencies of about 60% at a current density of 200 mA/cm^2 and high power densities (> 1 W/cm^2) in PEM fuel cells with high (4 mg/cm^2) or low (0.4 mg/cm^2) platinum loadings in electrodes. This article focuses on: (i) methods to obtain these high levels of performance with low Pt loading electrodes — by proton conductor impregnation into electrodes, localization of Pt near front surface; (ii) a novel microelectrode technique which yields electrode kinetic parameters for oxygen reduction and mass transport parameters; (iii) demonstration of lack of water transport from anode to cathode; (iv) modeling analysis of PEM fuel cell for comparison with experimental results and predicting further improvements in performance; (v) recommendations of needed R&D for achieving the above goals.

1. High energy efficiency and high power density fuel cell systems

1.1. Vital needs, essential criteria and candidate fuel cells

High energy efficiency and high power density fuel cells are vitally needed for extraterrestrial (space, underwater) and terrestrial (electric vehicles, standby or remote power, portable power source) applications to minimize fuel consumption, weight, volume and capital cost of power plants. The relative importance of energy efficiency and of power density depends on the application. In some cases, as for example, for a hydrogen energy storage system to be coupled with photovoltaic power plants for NASA's long lunar and Mars missions (14 days of darkness, 14 days of light), the energy efficiency is more critical than the power density because the weight of the energy storage sub-systems exceeds that of the fuel cell power conversion system by more than a factor of five. For military applications, where pulsed power is required, the power density is the over-riding factor. For the

0378-7753/91/$3.50

terrestrial transportation application, both the energy efficiency and power density have to be as high as possible.

The essential criteria for the attainment of high energy efficiencies and high power densities in fuel cells are: (i) low activation overpotentials which can be achieved by (a) using electrocatalysts with high exchange current densities for the oxygen reduction (ORR) reaction (the exchange current density for the hydrogen oxidation reaction is sufficiently high and thus activation overpotential losses due to this electrode reaction are minimal in all types of fuel cells); and (b) maximizing the electrochemically active surface areas; (ii) minimal mass transport overpotential, for example, by optimization of electrode structure to accelerate the transport of reactants to and products away from the active sites; and (iii) low ohmic overpotentials, for example, by minimization of the thickness of electrolyte layer and use of membranes with higher proton conductivities. All forms of overpotential can be reduced by operation at elevated temperatures and pressures. The fundamental limitation in fuel cells operating at low to intermediate temperatures (i.e., fuel cells with alkaline, phosphoric acid, proton exchange membrane electrolytes) is the low exchange current density for the oxygen reduction reaction, while in the higher temperature systems (molten carbonate and solid oxide), mass transport and ohmic overpotentials impede the attainment of high energy efficiencies and high power densities. In order to achieve high power densities, it is vitally important to minimize mass transport and ohmic overpotentials [1, 2].

The phosphoric acid fuel cell system, which is the most advanced fuel cell technology and close to commercialization for terrestrial applications, suffers from the problems of slow oxygen electrode kinetics, compared to that in alkaline and solid polymer electrolyte fuel cells. Thus, this system does not show promise for attainment of high energy efficiencies and high power densities. The molten carbonate and solid oxide fuel cells exhibit good oxygen electrode kinetics at the high operating temperatures of 650 and 1000 °C, respectively. However, the mass transport and ohmic problems are quite severe in these systems, thus making it difficult to attain both high energy efficiencies and high power densities. The only systems in which high energy efficiencies and high power densities have been simultaneously demonstrated are the alkaline and proton exchange membrane (PEM) fuel cells.

1.2. Demonstration of high power densities in alkaline and proton exchange membrane fuel cells

Significant progress has been made in achieving high energy efficiencies and high power densities in alkaline and proton exchange membrane fuel cells, particularly because (i) the ORR is considerably faster in these electrolytes than in any other electrolytes; (ii) the structures of the porous gas diffusion electrodes have been optimized to minimize mass transport overpotential; and (iii) very thin electrolyte layers are used to reduce ohmic overpotentials to negligible values. International Fuel Cells (IFC) has demonstrated that in advanced alkaline fuel cells the cell potential is as high as 1.0 V at 100

mA/cm^2 while it is 0.5 V at 8 A/cm^2 [2]. The high performances of the PEM fuel cells at Ballard Power Systems (BPS) may be represented by a cell potential of 0.9 V at 100 mA/cm^2 and 0.5 V at 6 A/cm^2 [3]. In the IFC and BPS fuel cells, the noble metal loading in the electrodes is quite high (≥ 4 mg/cm^2). Relatively high energy efficiencies and high power densities in PEM fuel cells with low platinum loading (≈ 0.4 mg/cm^2) electrodes (necessary for transportation applications) were demonstrated first at Los Alamos National Laboratory (LANL) and later at Texas A&M University (TAMU) by Srinivasan and coworkers [4, 5]. The best performance, reported by these workers to date, is 0.88 V at 100 mA/cm^2 and 0.62 V at 2 A/cm^2. In all the above cases, the pristine gases H_2 and O_2 were used as reactants. When using H_2/air as reactants in the fuel cells with low platinum loadings electrodes, the cell potential at 100 mA/cm^2 was 40 mV (the theoretical value) lower and at 2 A/cm^2 was 250 mV lower than when H_2/O_2 were used as reactants — the deviation from the theoretically expected value of 40 mV starts to occur at about 1.5 A/cm^2.

1.3. Methods of attainment of high power densities in proton exchange membrane fuel cells with low platinum loading electrodes

1.3.1. Extension of three-dimensional reaction zone by impregnation of proton conductor into active layer of electrode and hot-pressing of electrode to proton conduction membrane

An ingenious method, which was developed by Raistrick [6] to extend the three-dimensional reaction zone, is the impregnation of a proton conductor (say, Nafion®) into the active layer of the electrode (say, Prototech electrode with a platinum loading of 0.4 mg/cm^2). In this work, it was shown that such an electrode, mechanically pressed to a Nafion® membrane, exhibited a considerable improvement in oxygen reduction kinetics, as compared to that at an unimpregnated electrode/Nafion® interface. However, the first demonstration of high power densities in fuel cells with such impregnated electrodes was by Srinivasan *et al.* [7], who found it necessary to hot-press the electrodes onto the proton conducting membrane at a slightly higher temperature than the glass-transition temperature of the membrane and at a pressure of about 15 atm. Figure 1(a) and (b) illustrates the significant improvement in cell performance and the increase in electrochemically active surface area respectively by Nafion® impregnation of the electrode. This Figure also demonstrates the comparable performances and electrochemically active surface areas of single cells with high platinum loading and Nafion® impregnated low platinum loading electrodes.

1.3.2. Localization of platinum near front surface to minimize activation, mass-transport and ohmic overpotentials

From the cyclic voltammetric results, shown in Fig. 1(b), as well as from Rutherford Back Scattering experiments on a cross section of the electrodes, it was shown that the proton conductor penetrates only about 10 μm within the front surface. The active layer thickness in the state-of-

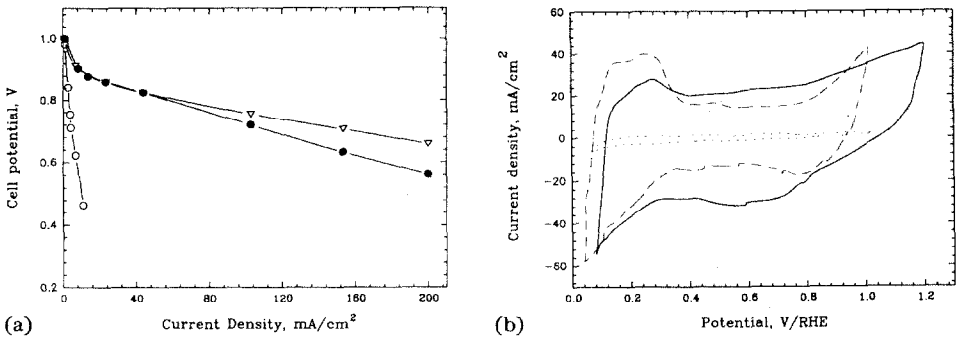

Fig. 1. (a) Cell potential/current density plots for H_2/O_2 fuel cells at 50 °C and 1 atm. pressure (electrodes 5 cm^2): (▽) and (○) Nafion®-impregnated and as-received Prototech electrodes (0.35 mg/cm^2 Pt) hot-pressed to Nafion® membranes; (●) GE/HS-UTC membrane and electrode (4 mg/cm^2 Pt). (b) Cyclic voltammograms on oxygen electrodes in fuel cells (electrodes 5 cm^2). (——) PEM D-120-cell with Nafion®-impregnated Prototech electrodes (0.35 mg/cm^2 Pt) hot-pressed to Dow membrane; (– – –) PEM #3-cell with GE/HS-UTC membrane and electrode assembly (4 mg/cm^2 Pt); and (-----) PEM #5-cell with as-received Prototech electrodes (0.35 mg/cm^2 Pt) hot-pressed to Nafion® membrane.

the-art low platinum loading electrodes (say, from Prototech or ETEK) is about 100 μm. These electrodes contain 10% Pt on carbon supports. In order to minimize activation, mass transport and ohmic overpotentials, which is vital for the attainment of high energy efficiencies and high power densities, Srinivasan and coworkers utilized (i) custom-made fuel cell electrodes with 20% or 40% (instead of 10%) platinum on carbon, while maintaining the same platinum loading (0.4 mg/cm^2); and (ii) sputter-deposited a thin layer of platinum (0.05 mg/cm^2) on the front surface of these electrodes [4]. The results of these studies, which are presented in Fig. 2 and Table 1 signify that (i) the platinum utilization of the electrodes is improved; and (ii) current densities of 1 A/cm^2 at a cell potential of 0.6 V can be achieved. It has recently been shown [5] that electrodes with thin layers of platinum, deposited using chemical or electrochemical techniques, yield performances close to those of the sputter-deposited electrodes (Fig. 3).

1.3.3. Use of thinner and alternate membranes

In most studies, which have been reported, DuPont's Nafion® 117 membranes (thickness of 175 μm) were used. To minimize ohmic and mass transport overpotentials in the membrane of a PEM fuel cell, two approaches, which were taken at LANL and TAMU, are the use of (i) thinner Nafion® membranes; and (ii) Dow® membranes with lower equivalent weight. Typical results are presented in Fig. 4. The cell with the 50 μm thick Nafion® membrane exhibits the highest cell potential at 2 A/cm^2. However, the open-circuit potential in this cell was 50–100 mV lower than in the cells with the other membranes because of cross-over of the hydrogen gas. The cross-over

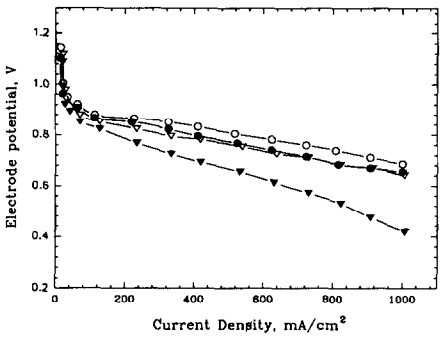

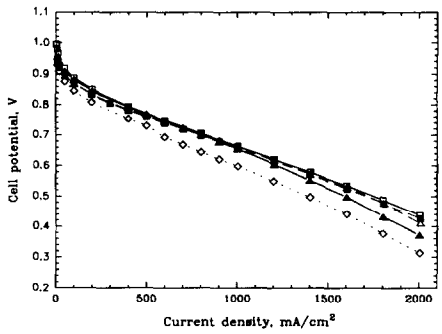

Fig. 2. Effect of localization of Pt near the front surface of Prototech electrodes on the performance of oxygen electrode in H_2/O_2 single cell at 80 °C and at 3/5 atm. (▽) 40 wt.% Pt/C plus 50 nm sputtered film of Pt; (○) 20 wt.% Pt/C plus sputtered film of Pt; (●) 20 wt.% Pt/C; and (▼) 10 wt.% Pt/C. The H_2 counter electrode in each case was the same as the working electrodes [4].

Fig. 3. Cell potential vs. current density plots for single cells with electrodes having localized Pt layer deposited by different methods, all operating at 95 °C and with H_2/O_2 at 4/5 atm. (□) H_2PtCl_6 brushed, (■) Pt in Nafion® sol., (△) electroplated Pt, (▲) sputtered Pt, (◇) control Prototech electrode.

TABLE 1

Effects of localization of platinum near front surface of electrode on hydrogen adsorption charge and roughness factor as determined by cyclic voltammetry and on percentage of platinum utilization

Method of Pt localization	Q_H (mC cm^{-2})	Roughness factor[a]	Utilization of Pt[b] (%)
10% Pt/C	4.4	20	4
10% Pt/C+50 nm Pt film	9.6	44	9
20% Pt/C	11.4	53	11
20% Pt/C+50 nm Pt film	15.3	70	14
40% Pt/C	17.0	77	15
40% Pt/C+50 nm Pt film	19.2	87	17

[a]Calculated assuming 220 μC/cm^2 for Q_H on smooth Pt.
[b]Estimated assuming a 2.0 nm particle size for the Pt on C catalyst, as was shown by electron microscopy of the materials. % of Pt utilization = (roughness factor/total Pt surface area ×100).

effect is also reflected by a lower potential in the cell with the 50 μm thick membrane than in the cell with a 175 or 100 μm thick membrane, at low current densities. The cell with the Dow® membrane, 125 μm thick, showed the next best result. Due to its lower equivalent weight than that of Nafion®, it has a better conductivity and water retention capability. It is also striking that the cells with the Nafion® membrane (thicknesses 100 and 175 μm) encounter mass transport limitations at higher current densities but the cell with the Dow® membrane does not.

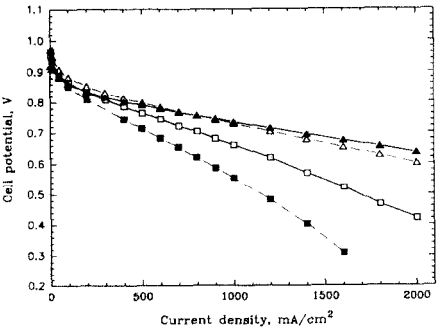

Fig. 4. Cell potential vs. current density plots for single cells with different membrane materials, operating at 95 °C with H_2/O_2 at 4/5 atm. Pt loading on each electrode: 0.45 mg/cm^2 [5]. (▲) Nafion® 50 μm, (△) Dow 125 μm, (□) Nafion® 100 μm, (■) Nafion® 175 μm.

2. Oxygen electrode kinetics at platinum/Nafion® interface

2.1. Tafel parameters on microelectrode from slow potential sweep and electrochemical impedance spectroscopic experiments

The objectives of this work [8] were to determine the electrode kinetic parameters for the reduction of oxygen at the Pt/Nafion® interface under totally solid state conditions (i.e. no contacting liquid electrolyte phase). Thus, these investigations were carried out under the same conditions as in a practical fuel cell. The concentration and diffusion coefficient of oxygen in Nafion® were also determined. Earlier studies of the platinum/solid polymer electrolyte interface, using platinum gauze electrodes, indicated that kinetic information was masked by large contributions from ohmic and mass transport effects [9]. Such problems were addressed in this investigation by using a novel solid state cell, incorporating a platinum microelectrode (Fig. 5). Cyclic voltammetric and potentiostatic transient measurements were made at the Pt/Nafion® interface. From the high scan rate cyclic voltammetric experiments, the purity of Nafion® and of the electrode was ascertained and the roughness factor of the electrode was calculated. The slow sweep experiments yielded the Tafel parameters for oxygen reduction. From the two-section Tafel plot (Fig. 6), the exchange current densities were calculated and found to be higher than those obtained at any other Pt/acid interface. The electrode kinetic parameters obtained therefrom are presented in Table 2.

These results were also substantiated by electrochemical impedance spectroscopic (EIS) investigations [10]. A typical impedance plot (Nyquist plot) at the open-circuit potential is shown in Fig. 7. From the charge transfer resistance R_{ct} at this potential, one can calculate the corrosion current density according to eqn. (1)

$$R_{ct} = \frac{RT}{n\, i_{corr} F} \tag{1}$$

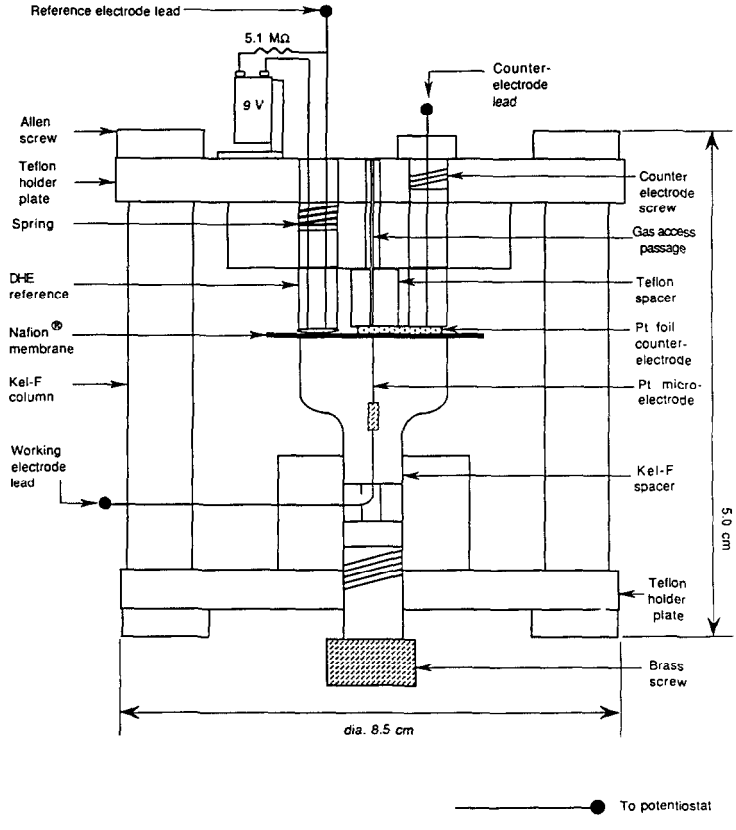

Fig. 5. Schematic of the solid state cell incorporating a platinum microelectrode [8].

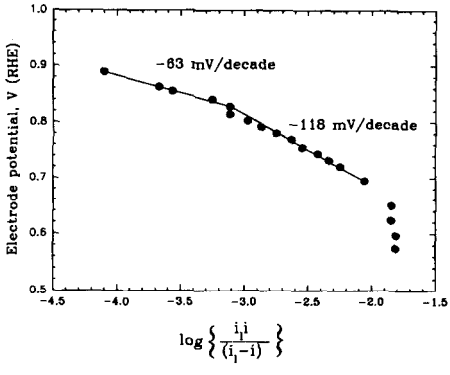

Fig. 6. Mass transfer corrected Tafel plot for oxygen reduction at the platinum microelectrode/ Nafion® interface, at 25 °C [8].

TABLE 2

Electrode kinetic parameters for oxygen reduction at the Pt/Nafion® interface using fuel cell electrodes and microelectrodes

Electrode/membrane interface at 50 °C, 1 atm. pressure	Tafel slope b (mV/dec)	Exchange current density, i_0 (A/cm^2)[a]
Unsupported Pt black (10 mg/cm^2 on carbon cloth) (ElectroChem Inc.)/125-μm Dow membrane	−58	3.09×10^{-7} r.f. 773
Platinum supported on carbon (20%Pt/C), Pt loading 0.4 mg/cm^2; Nafion® impregnated 0.4 mg/cm^2 (Etek, Inc.)/ 125-μm Dow membrane	−64	1.09×10^{-7} r.f. 52
100-μm Pt microelectrode/175-μm Nafion® at 25 °C, 1 atm. pressure;	−63	2.05×10^{-9}
pseudo-steady state voltammetry	−118	7.8×10^{-7}
100-μm Pt microelectrode/175-μm Nafion® at 25 °C, 1 atm. pressure;	−65	4.09×10^{-8}
electrochemical impedance spectroscopy	−133	5.9×10^{-7}

[a]Normalized for electrochemically active surface area; r.f. roughness factor.

The corrosion current density (i_{corr}) corresponds to the current density for oxygen reduction, as well as that for the platinum oxide formation, at the open-circuit potential. From EIS measurements over a range of potentials and a plot of log R_{ct} versus current density, the Tafel slope which was obtained was found to agree with the results of the pseudo-steady state method (Table 2). From the values of i_{corr} and Tafel slope, the exchange current density for oxygen reduction on the platinum microelectrode was calculated; its value was consistent with that obtained by the pseudo-steady state method (Table 2).

2.2. Tafel parameters on fuel cell electrodes from galvanostatic measurements

Electrode kinetic studies of oxygen reduction in PEM fuel cells (single cells) have been conducted at LANL since 1986 and at TAMU since 1988. A systematic study of ORR kinetics in fuel cells, as a function of temperature and pressure was recently carried out at TAMU. The fuel cell electrodes contained either high (4–10 mg/cm^2) or low ($\approx$0.4 mg/cm^2) platinum loadings. The plot of the potential of the oxygen electrode with respect to the reversible hydrogen electrode potential, as well as that of the single cell versus the current density fits eqn. (2)

$$E = E_0 - b \log i - Ri \tag{2}$$

where

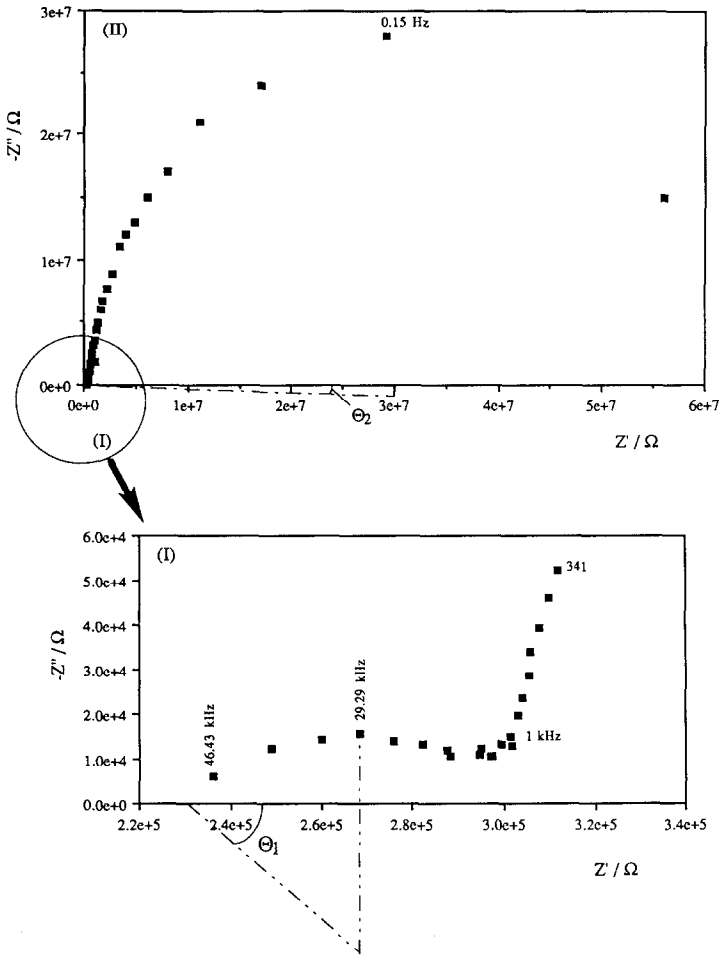

Fig. 7. Nyquist plot obtained at open circuit potential at the platinum/Nafion® interface showing charge transfer relaxation; inset shows high frequency membrane relaxation process [10].

$$E_0 = E_r + b \log i_0$$

and E_r is the reversible potential for the half or single cell; i_0 and b are the exchange current density and Tafel slope for the ORR and R represents the resistance (predominantly ohmic as well as the charge transfer resistance for the hydrogen electrode) which causes a linear variation of the potential with current density. The Tafel plots for ORR in single cells with high and low platinum loading electrode at 50 °C are presented in Fig. 8. From such plots, the exchange current densities (based on geometric areas of electrodes) and Tafel slopes were determined. In these experiments, cyclic voltammograms were also recorded on the electrodes; from the coulombic charge required for hydrogen adsorption or desorption, the electrochemically active surface

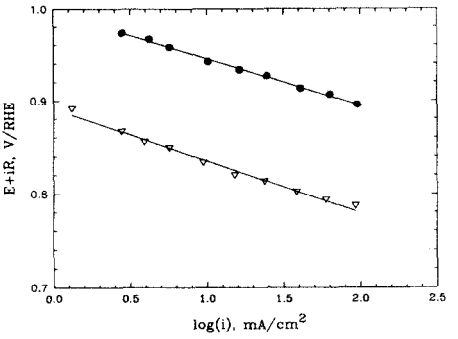

Fig. 8. *iR* corrected Tafel plots for oxygen reduction at membrane electrode assemblies using unsupported (●) and supported (——) platinum gas diffusion electrodes [11].

areas and hence of the roughness factors of the electrodes were calculated. Using these roughness factors, the exchange current densities, based on the real surface area of the electrode were obtained. Table 2 also illustrates a comparison of the electrode kinetic parameters for ORR on fuel cell electrodes at 50 °C and on the microelectrodes at 25 °C. The fuel cell electrodes exhibit only the low Tafel slope, 60 mV/decade, because even at the high current density of 2 A/cm^2 (based on geometric areas of the electrode) the half cell potential is still in the platinum oxide covered region, where the low Tafel slope is observed on smooth platinum microelectrode. The exchange current densities (based on the real surface area of the platinum) are nearly the same on the fuel cell electrode and on the microelectrode. More details of this work, including that of the effects of pressure and temperature will be published shortly [11].

3. Mass transport and ohmic phenomena

3.1. Oxygen solubility and diffusion coefficient in proton exchange membrane from microelectrode experiments

The microelectrode technique is a unique method for determining the electrode kinetic parameters (as described in Section 2.1) and mass transport parameters. It involves chronoamperometry — the potential of the microelectrode is stepped from a value where no oxygen reduction occurs (open-circuit potential) to that at which oxygen reduction occurs at the limiting current density. According to microelectrode theory [12], the dependence of the current density (i) on time (t) for such an experiment follows eqn. (3)

$$i = \frac{nF\pi^{1/2}D^{1/2}Cr^2}{t^{1/2}} + \pi nFDCr \tag{3}$$

where n is the number of electrons transferred in the overall reaction ($n=4$ for ORR); D and C are the diffusion coefficient and solubility of oxygen in

the PEM; and r is the radius of the microelectrode. Thus, a plot of i versus $t^{1/2}$ is linear and from the values of the slope and of the intercept, the diffusion coefficients and solubilities can be easily calculated. It must be noted that this is not the case when transient methods (a.c. impedance, cyclic voltammetry) are used on macroelectrodes. In these cases, only the product $D^{1/2}C$ is obtained and unless some other method can be used to find D or C independently, the two values cannot be individually determined. A typical plot of i versus $t^{-1/2}$ for ORR on Pt in Nafion® is shown in Fig. 9 [8]. The values of the diffusion coefficient and solubility, calculated from this plot are presented in Table 3. The difference between these values and those reported by other workers are probably due to different experimental conditions — water content of membrane, measurements with other acids in membrane, etc.

3.2. *Dependence on temperature and pressure*

Both the temperature and pressure of operation of the cell have a significant influence on its performance. The effect of temperature on performance is illustrated in Fig. 10 for four temperatures from 50 to 95 °C at a pressure of 5 atm. The slope of the linear region of the cell potential versus current density plot decreases, which is indicative of a lowering of the internal resistance of the cell; this decrease is predominantly due to the

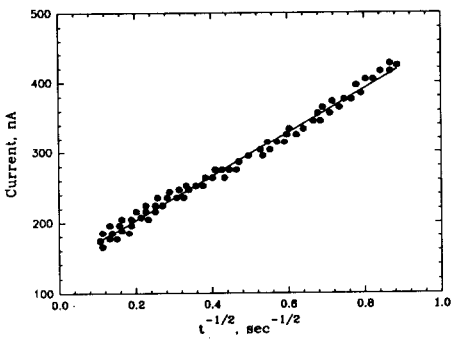

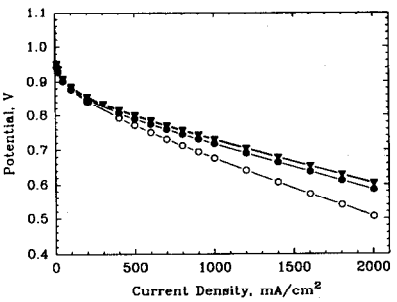

Fig. 9. Current vs. $t^{-1/2}$ plot at the platinum/Nafion® interface to determine mass transport parameters of oxygen in Nafion® [8].

Fig. 10. Effects of temperature on the performance of a PEM H_2/O_2 fuel cell, Pt loading of electrodes 0.45 mg/cm², Dow membrane, 5 atm. (▼) 95 °C, (▽) 85 °C, (●) 70 °C, (○) 50 °C.

TABLE 3

Transport parameters for oxygen in Nafion from measurements at Pt/microelectrode interface

Diffusion coefficient, D (cm²/s)	7.4×10^{-7}
Solubility, C (mM/l)	26

decrease in the ohmic resistance of the electrolyte. The mass transport limitations, caused by the diffusion of reactants through the PEM assembly to the active Pt sites, the movement of the protons from the anode to the cathode and the removal of product water, are also reduced with the increase of temperature. At a cell temperature of 95 °C and pressure of 5 atm., it has recently been shown in our laboratory that the linear region extends to over 3 A/cm^2, indicating that the mass transport limitations are minimal up to this current density.

3.3. Dependence on cathodic reactant — oxygen versus air

By necessity, the source of oxygen for terrestrial applications is air and it is the pure gas (cryogenic of compressed gas) for extraterrestrial (space, underwater) applications. Experiments using both these gases in single cells, operating in the temperature range of 25 to 95 °C and at pressures from 1 to 5 atm., show the striking influences of mass transport phenomena in the cell and half cell potential versus current density plots (Figs. 11 and 12). Figure 11 demonstrates the effect of pressure at 50 °C, while Fig. 12 represents the effect of temperature, at a pressure of 5 atm. on the cell potential versus current density plot using H_2/O_2 and H_2/air as reactants. Two effects are apparent on passing over from oxygen to air as the cathodic reactant: (i) the slope of the linear region of the E–i plot is 50% higher; and (ii) deviations from the linear region are visible at lower current densities. In the higher temperature fuel cells (phosphoric, molten carbonate, solid oxide) the oxygen gain in potential is constant at all current densities in the linear region and thus the slopes of the E–i plot are the same with H_2/O_2 and H_2/air as reactants. The dependence of the slope of the E–i line on the oxygen partial pressure is indicative of mass transport limitations, which also cause a linear variation of E with i at lower current densities. It is very probable that there is a 'nitrogen barrier layer effect' which causes

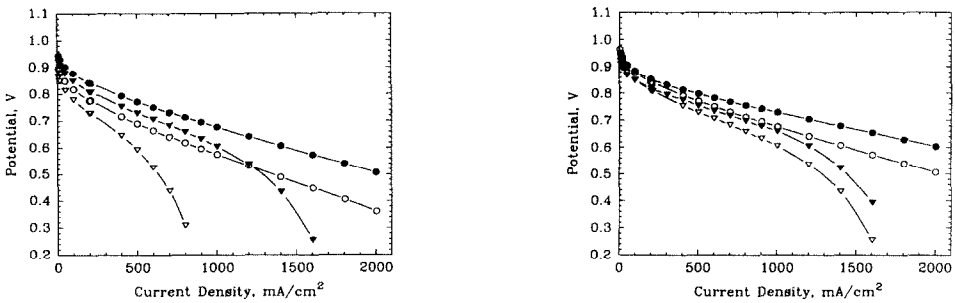

Fig. 11. Effect of pressure and reactant gas on the performance of a PEM fuel cell, Pt loading of electrodes 0.45 mg/cm^2, Dow membrane, 50 °C. (●) 5 atm. O_2, (○) 1 atm. O_2, (▼) 5 atm. air, (▽) 1 atm. air.

Fig. 12. Effect of temperature and reactant gas on the performance of a PEM fuel cell, Pt loading of electrodes 0.45 mg/cm^2, Dow membrane, 5 atm. (●) 95 °C oxygen, (○) 50 °C oxygen, (▼) 95 °C air, (▽) 50 °C air.

this mass transport limitation. In a previous study, it was also shown that the dependence of the cell potential (E_P) on pressure (P) at a constant current density may be expressed by eqn. (4)

$$E_P = E_1 + b \log P \tag{4}$$

where E_1 is the cell potential at 1 atm. and b is the Tafel slope for the reaction. The derivation of this equation is based on a reaction order of unity for the ORR. This equation is valid over the entire region of P investigated with oxygen, but when using air at pressures between 1 and 1.5 atm. there is a more rapid increase of E with P.

The second effect, i.e. deviations from the linear region of the E versus i plot at lower current densities with air than with oxygen is clearly due to the effect of partial pressure of oxygen. The 'nitrogen barrier layer effect' could still play a role. A challenge is to operate a cell at least at 2 A/cm^2 and a cell potential above 0.5 using steam-reformed hydrogen and air as reactants. Optimization of the structure of the electrode to minimize mass transport limitations is essential.

3.4. Dependence on thickness and conductivity of membrane

The spade work on proton exchange membrane fuel cells has been carried out using DuPont's Nafion® 1100 as the electrolyte layer. Nafion® membranes, with different thicknesses (50, 100 and 175 μm) have been incorporated as the proton exchange membrane in single cells and their performances determined (see Section 1.3.3). As one may expect, the thinner the membrane, the lower is the slope of the linear region of the cell potential versus current density plot (Fig. 4). However, another significant effect is that mass transport limitations are greatly reduced or even eliminated by using thinner membranes. The mass transport effects are clearly due to phenomena within the membrane — water and/or proton transport.

The emerging proton exchange membrane for fuel cells is the one manufactured by Dow Chemical Company with a lower equivalent weight than that of Nafion® 1100. The chemical structures of the DuPont and Dow membranes are illustrated in Fig. 13. The presence of more sulfonic acid groups per CF_2 in the Dow membrane than in Nafion® enhances the electrolyte conductivity and water retention capability. A well humidified membrane in PEM fuel cells is vital as otherwise problems of increase in electrolyte resistance and consequent loss in performance are encountered. Figure 4

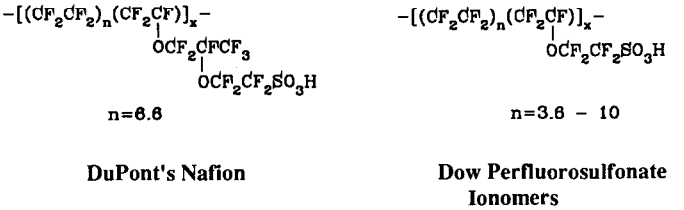

Fig. 13. The skeleton structure of Dupont's Nafion® and Dow's perfluorosulfonate membrane.

also shows that the cell with the Dow membrane (thickness 125 μm) shows a lower slope in the linear region of the E–i plot than that in the cell with the Nafion® membrane (thickness 100 μm). Further, mass transport limitations are visible at high current densities in the latter but not in the former cell. The higher conductivity and the better mass transport (proton and water) capabilities of the Dow membranes are reflected in Fig. 4.

3.5. Evidence for lack of net water transport from anode to cathode

It has been reported that in the PEM fuel cell, a proton crossing the membrane carries with it four to six water molecules. In the present study, the amount of water transported across the membrane during the cell operation was measured in order to evaluate more accurately the mass balance conditions in the cell [13]. A PEM fuel cell with a 50 cm^2 electrode geometric area was used in the experiments with two different types of proton conducting membranes — Nafion® from DuPont and Dow experimental type. The electrodes used in this study were supplied from Prototech, Inc., and contained 20% Pt on carbon (0.4 mg/cm^2) on a carbon cloth substrate. Details of the experimental set up are published elsewhere [5]. In these experiments, the oxygen gas entering the cell was dry. The hydrogen gas was saturated with water vapor. The gas exiting the cell from the cathode chamber was passed through a condenser consisting of a copper spiral immersed in iced-water. The water exiting the condenser was collected and its rate calculated. The results of experiments with a Dow experimental type membrane (125 μm thick) are presented in Fig. 14. The solid line presents the rate of water production corresponding to Faraday's law. The points represent the experimentally measured collection rates. At low current densities, the measurements are not very accurate because of the long period of time needed to collect measurable amounts of water. As can be seen from Fig. 14, the amount of water produced at atmospheric pressure and 50 °C corresponds to Faraday's law. There are two possible explanations for this effect. The first is that there is no water transport across the membrane and that the proton transport is by a hopping mechanism (Grothus conduction). The second one is that due to the concentration gradient of water, which will

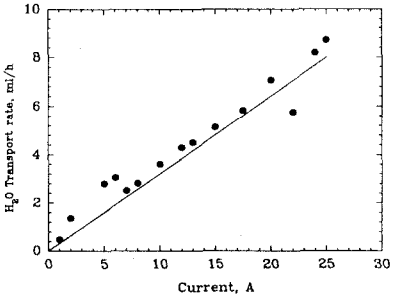

Fig. 14. Water production rate in a 50 cm^2 area PEM H_2/O_2 fuel cell with Dow membrane, 50 °C, 1 atm. (——) Faraday's law, (●) measured.

be set up during current flow, the back-diffusion of water compensates for the water molecules dragged with the protons. The first explanation is the most likely one. Experiments are underway to determine if there is water transport across the membrane at higher operating temperatures and pressures (3–5 atm.), which are necessary to attain the high power densities required of fuel cells for transportation, space and defense applications.

4. Prognosis of attainable energy efficiency and power densities

4.1. Best performances obtained with high and low platinum loading electrodes

The cell potential versus current density plot up to the end of its linear region fits eqn. (2). In Table 4 are presented the values of E_0, b and R, evaluated by non-linear least-squares fits to the experimental points, for the cells exhibiting high levels of performance: cells with (i) high platinum loading (10 mg/cm^2) electrodes and 125 μm thick Dow membranes (Fig. 15);

TABLE 4

Electrode kinetic parameters for PEM H_2/O_2 fuel cells, as evaluated by non-linear least squares fit of experimental results. Also included are current densities at cell potential of 0.9 V. Temperature 85 °C, pressure 5 atm.

Electrode, platinum loading, membrane	E_0 (V)	b (V/decade)	R (Ω cm^2)	$i_{0.9}$ (A/cm^2)
Electrochem, Inc., 10 mg/cm^2 Dow membrane, 125 μm	1.065	0.055	0.110	300
Prototech, 0.4 mg/cm^2 Nafion® 175 μm	1.007	0.046	0.298	70
100 μm	1.008	0.045	0.201	61
Dow membrane, 125 μm	1.002	0.053	0.111	62

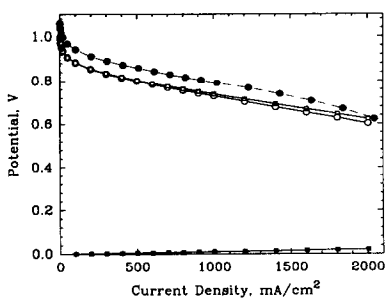

Fig. 15. Half cell and single cell performance of PEM H_2/O_2 fuel cell, 95 °C, Dow membrane, 5 atm. (●) E_{cell} for 10 mg/cm^2 Pt loaded electrodes, (○) E_{cell} for 0.45 mg/cm^2 Pt loaded electrodes, (□) E_{O_2} for 0.45 mg/cm^2 Pt loaded electrodes, (■) E_{H_2} for 0.45 mg/cm^2 Pt loaded electrodes.

(ii) low platinum loading electrodes and 125 μm thick Dow membranes (Fig. 4); and (iii) low platinum loading electrodes and Nafion® membranes with thicknesses of 100 or 175 μm (Fig. 4). The current densities at a cell potential of 0.9 V are also presented in Table 4. All these cells were operated at 85 °C and 5 atm. pressure. Table 4 illustrates that E_0 is generally approximately equal to 1.0 V, b is between 0.05 and 0.06 V/decade and R is between 0.1 and 0.3 Ω cm^2. The electrochemically active surface area is about 10 times higher for the high platinum loading than for the low platinum loading electrode, even though the platinum content in the former case is 20 times higher than in the latter. The effective utilization of the platinum is about 5% for the cell with the high platinum loading electrodes and about 10% for the ones with low platinum loading electrodes. It is also worthwhile noting the the current density in the predominantly activation-controlled region, based on the electrochemically active surface area of the electrodes, is approximately the same for the cells with the high and low platinum loading electrodes. In order to attain high power densities, the value of R has to be as low as possible, as in the case 125 μm thick Dow membrane.

4.2. Prediction of performance improvements — modeling analysis

Since eqn. (2) is quite representative of the cell potential versus current density plot up to the end of the linear region, a simplified modeling analysis was carried out to determine the effects of the parameters E_0, b and R. The results of this analysis are presented in Fig. 16(a)–(c). Figure 16(a) shows that increase of the value of E_0 (for constant b and R values) causes a parallel shift of the cell potential versus current density plot and thus for a 50 mV increase, the energy efficiency is increased by about 4%. This Figure also shows that the power density can be significantly improved by higher values of E_0. However, the power density is also influenced by the value of R. For $R = 0.1$ Ω cm^2, which value was used for the plots in Fig. 16(a), the current density at a cell potential of 0.8 V increases by a factor of only two when E_0 increases from 1.0 to 1.05 V, whereas it will be close to one order of magnitude higher if R were equal to zero (i.e. when fuel cell is only activation-controlled). It must be noted that E_0 is expressed by eqn. (2) and hence the basic parameter which determines E_0 is the exchange current density for the ORR (based on the geometric area of the electrode). Two possible approaches to increase i_0 are (i) finding better electrocatalysts; and (ii) increasing the effective utilization of platinum. E_0 can also be increased by increasing the value of E_r, the thermodynamic reversible potential. Operation at higher pressures is the only way of obtaining a higher E_r. The Nernst equation shows that for a ten fold increase of pressure, E_r increases for the hydrogen/oxygen fuel cell by 45 mV.

According to eqn. (2) if the current density is expressed in mA/cm^2, E_0 is the value of E at 1 mA/cm^2 (geometric). At this current density the contribution of ohmic overpotential to the cell potential is negligible. The current density, based on the electrochemically active surface area of the electrode is about fifty times lower than that based on the geometric area

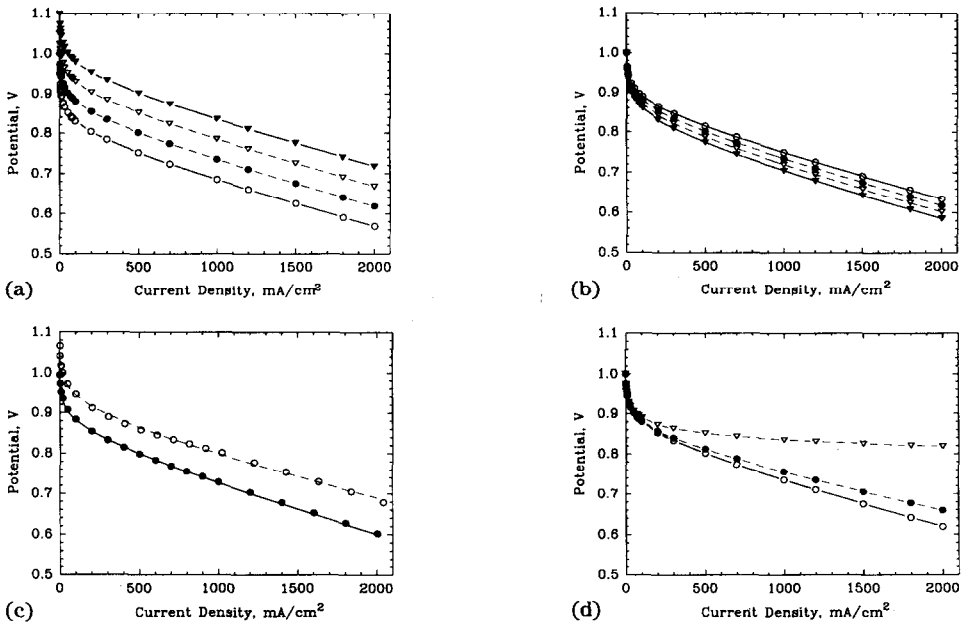

Fig. 16. Cell potential–current density plots: (a) to (c) modelling analysis; (d) least-squares fit of experimental results in PEM H_2/O_2 fuel cell, 95 °C, 5 atm. (a) $R = 0.10\ \Omega\ cm^2$, $b = 55$ mV/dec, (▼) $E_o = 1.100$ V, (▽) $E_o = 1.050$ V, (●) $E_o = 1.000$ V, (○) $E_o = 0.950$ V; (b) $E_o = 1.00$ V, $R = 0.10\ \Omega\ cm^2$, (○) $b = 50$ mV/dec, (●) $b = 55$ mV/dec, (▽) $b = 60$ mV/dec, (▼) $b = 65$ mV/dec; (c) $E_o = 1.00$ V, $b = 55$ mV/dec, (▽) $R = 0.0\ \Omega\ cm^2$, (●) $R = 0.08\ \Omega\ cm^2$, (○) $R = 0.10\ \Omega\ cm^2$; (d) calculated vs. experimental data, (○) 10 mg/cm² Pt, (– – –) $E_o = 1.08$ V, $b = 62$ mV/dec, $R = 0.09\ \Omega\ cm^2$, (●) 0.5 mg/cm² Pt sputtered, (——) $E_o = 1.00$ V, $b = 55$ mV/dec, $R = 0.11\ \Omega W\ cm^2$.

for the cell with the low platinum loading electrodes and 500 times lower for the one with high platinum loading electrodes. At these low values of current densities, the value of E_0 will be very close to that of the open circuit potential. The open circuit potential is a mixed potential involving oxygen reduction as the cathodic reaction and the platinum oxide formation (and to a small extent platinum dissolution) as the anodic reaction. When using carbon in the active layer of the electrode, as with supported electrocatalysts, the electrochemical oxidation of the carbon also influences the open circuit potential. This is one of the main reasons for the E_0 values being lower for electrodes with supported than with unsupported electrocatalysts. A problem, which may thus arise by attaining higher E_0 values, is that the rates of the above mentioned anodic reactions will increase and cause degradation of the structure of the electrode and hence of performance.

Figure 16(b) shows the effect of variation of the Tafel slope for the ORR on the cell potential versus current density plot. The values of the Tafel

slope chosen are in the range of those experimentally observed. The lower the Tafel slope, the better is the performance and it is more significant at higher current densities because the slope of the cell potential versus current density plot increases with increase of the Tafel slope. The Tafel slope of 60 mV/decade is representative of oxygen reduction on the oxide covered platinum in acid medium [14], including the PEM [8]. Tafel slopes, lower than the assumed values, have rarely been observed for oxygen reduction. One can expect lower Tafel slopes if an intermediate step, further down the reaction sequence, say after 2 of the 4 electrons have been transferred to the oxygen molecule, is the rate-determining step [15]. An alternative mechanism which could yield low Tafel slopes is via redox catalysis which may be possible by use of alloys such as PtCr, PtCo, PtNi, etc., where the electrochemical reaction is the reduction of the transition metal ion from a higher valence state to a lower one and oxygen chemically oxidizes the lower valent metal ion to the higher one.

The most difficult challenge in achieving higher power densities is exemplified in Fig. 16(c), i.e., the marked effect of R, which represents the effective resistance causing a linear variation of overpotential (predominantly ohmic) with current density. As stated in Section 3.4, the best performance has been achieved in the single cell with the Dow membrane and hence in Fig. 16(c), the highest R value used is that for the best performing cell (Fig. 4). The other extreme is for the case when $R = 0$), which is a hypothetical case, where the overpotential loss is only due to activation control of the ORR. The intermediate value chosen is $R = 0.08\ \Omega\ cm^2$. The corresponding values of the cell potential at a current density of 2 A/cm^2 are 0.80, 0.60 and 0.64 V, respectively. The assumption that $R = 0$ is invalid because R includes at least the contributions of the ohmic resistance of the electrolyte layer and of the charge transfer resistance of the hydrogen oxidation reaction. Further, it will be extremely difficult to completely eliminate resistances of contacts, including bipolar plates in multi-cell stacks. Assuming that (i) these resistances are negligible; (ii) the electrolyte resistance is 0.05 $\Omega\ cm^2$ (using a specific resistance of 5 Ω cm and thickness of 100 μm for the electrolyte); and (iii) the charge transfer resistance for hydrogen oxidation is 0.025 $\Omega\ cm^2$ (which is the best value obtained in our laboratory) the total value of R is 0.075 $\Omega\ cm^2$ (i.e., very close to the assumed intermediate value of 0.08 $\Omega\ cm^2$). This brief analysis gives a realistic estimate of a cell potential of 0.64 V at a current density of 2 A/cm^2, corresponding to an energy efficiency of 43% and a power density of 1.28 W/cm^2 (assuming $E_0 = 1.0$ V and $b = 0.055$ V/decade). The maximum power density for this cell will be about 3 W/cm^2. If, however, E_0 is 1.10 V instead of 1.0 V, the cell potential will increase to 0.74 V at 2 A/cm^2 and thus the energy efficiency and power density as this current density will be 50% and 1.48 W/cm^2.

Figure 16(d) shows the validity of the present treatment for the best performances achieved in single cells with high and low platinum loading electrodes. There is close agreement between the results of the numerical simulation and experimental results.

4.3. Needed research and development to attain projected performance levels

4.3.1. Increase of platinum utilization and use of alloy electrocatalysts

One of the main contributions to the loss in efficiency and power density in PEM fuel cells is the activation overpotential at the cathode, which is highly visible from the cell and half cell performance in Fig. 15 (single cell with electrodes having a Pt loading of 0.45 mg/cm^2). This Figure also shows that, over the entire current density range, the potentials in a cell with the high platinum loading electrodes are about 50 mV higher at all current densities than those in a cell with low platinum loading electrodes. However, because of the vital importance to develop fuel cells with low platinum loading electrodes, a two-pronged attack should be followed: (i) increase the effective utilization of platinum, at least by a factor of 2 over the present value ($\approx$ 10%); and (ii) use alloy electrocatalysts with higher exchange current densities. Possible approaches for the former are use of (i) still thinner active layers with a higher percent platinum on carbon (say, 40% Pt/C); and (ii) vacuum-impregnation or incorporation of the proton conductor (during fabrication) into the electrode to further extend the three-dimensional reaction zone. In the case of the latter, alloys of platinum with Co, Cr or Ni, which have been successfully used to enhance oxygen reduction kinetics in phosphoric acid fuel cells, need be evaluated [16].

4.3.2. Optimization of structure of electrode and of membrane and electrode assembly to minimize mass transport and ohmic overpotentials with air as reactant

One of the challenges in PEM fuel cells is to minimize mass transport and ohmic overpotentials. As seen from Figs. 11 and 12, when using hydrogen/air rather than hydrogen/oxygen as reactants, the slopes of the linear region in the cell potential versus current density plots are about 50% higher. Further, these Figures show that at higher densities mass transport limitations are encountered with H_2/air as reactant, but not with H_2/O_2. To minimize these rate-controlling processes, optimizations of the structure of the electrode and of the membrane and electrode assembly are essential. Possible solutions are: (i) altering the Teflon content of the electrode; (ii) use of electrodes with thinner diffusion and active layers; (iii) incorporation of a proton conductor during the fabrication of electrodes.

4.3.3. CO-tolerant electrocatalysts for hydrogen oxidation and methanol oxidation electrocatalysts

In the above sections, hardly any mention has been made about necessary improvements in the hydrogen electrode, because most of the experimental results quoted are when pristine hydrogen is used as the anodic reactant and oxygen or air is the cathodic reactant. Pure hydrogen and oxygen are, invariably, the reactants for extraterrestrial applications. However, for transportation and other terrestrial applications where PEM fuel cells will be used,

methanol is presently the fuel of choice. Because of the low activity of the best electrocatalysts for methanol oxidation, the indirect route (reformer-fuel cell) is most promising for the near to intermediate term time-frame (say, up to the year 2010). The CO content of the reformed fuel is 1%, which cannot be tolerated by the anode. Ballard Power Systems made excellent progress in reducing this value to about 100 ppm by selective oxidation – passing the reformed gas with 1% to 2% oxygen over a platinum/alumina catalyst at 160 °C. Even 100 ppm of CO poisons the platinum anode, but platinum/ruthenium alloy electrocatalysts are tolerant to this level of CO. It is essential that investigations be made on alloy electrocatalysts and/or oxide supports, which enhance CO oxidation and reduce the poisoning problem.

Finding CO tolerant electrocatalysts and/or oxide supports may also fulfil the 'fuel cell researcher's dream' – the direct oxidation of methanol in fuel cells. FT-IR studies reveal that the intermediate which is formed during methanol oxidation and causes a poisoning problem, appears to be the same as the poisoning species adsorbed from carbon monoxide [17]. Potential electrocatalysts for methanol oxidation, which are of the redox type (i.e. electrochemical oxidation of the metallic species to a higher valence state, which chemically oxidizes the methanol) are Pt–Ru, Pt–Sn, Pt–Mo alloys.

5. Concluding remarks

The conclusions which may be drawn from this article may be summarized as follows.

(i) PEM and alkaline fuel cells are the strongest candidates for achieving high energy efficiencies and high power densities, vitally needed for extra-terrestrial and terrestrial applications. The PEM fuel cell has the advantage over the alkaline fuel cell because of CO_2 tolerance and longer lifetimes.

(ii) Significant progress has been made in the attainment of high energy efficiencies and high power densities in PEM fuel cell with high (4.0 mg/cm^2) and low (0.4 mg/cm^2) platinum loading electrodes.

(iii) Novel approaches have been used in PEM fuel cells with low Pt loading electrodes to attain the same levels of performance as those with high Pt loading: (a) proton conductor impregnation into the electrode; (b) optimized conditions for the hot-pressing of electrodes to PEM's and of pressure and temperature; (c) localization of platinum near the front surface; (d) use of thin membranes with better conductivity and water retention capability.

(iv) Electrode kinetic and mass transport parameters for ORR at a Pt/PEM interface were determined using a Pt microelectrode and pseudo-steady state, transient and impedance spectroscopic techniques. Values of the electrode kinetic parameters are comparable on the smooth microelectrodes and high surface area fuel cell electrodes.

(v) The absence of net water transport from anode to cathode was demonstrated.

(vi) A modeling analysis was carried out to demonstrate that the performance levels obtained in PEM fuel cells are approaching those projected, which are based on realistic values for the electrode kinetic and ohmic parameters.

(vii) In order to achieve the projected performance levels, it is necessary to (a) improve the effective utilization of platinum from 10% to about 50% and/or use Pt alloy electrocatalysts for the ORR; (b) find membranes with better conductivity; and (c) discover CO tolerant electrocatalysts for hydrogen oxidation and electrocatalysts with a high activity for the direct oxidation of methanol — the latter is the 'fuel cell researcher's dream'. Both these areas are vitally important for the transportation application.

Acknowledgements

The authors wish to express their sincere appreciation to Dr Edson Ticianelli of the University of São Paulo at São Carlos, Mr Charles R. Derouin of Los Alamos National Laboratory and Dr Mohammad A. Enayetullah of Johnson Matthey, Inc., who made significant contributions to the work carried out at LANL and/or TAMU. The research work at LANL was sponsored by the U.S. Department of Energy and at TAMU by the Defense Advanced Research Project Agency, Energy Research Application Program — Texas Higher Education Coordinating Board, Electrochem, Inc., Center for Space Power — TAMU and NASA Johnson Space Center. The authors are also grateful to the Dow Chemical Company (Drs Jeffrey A. Gunsher, Glenn A. Eisman and Alan Cisar) and DuPont Chemical Company (Dr Walther Grot) for providing the proton exchange membranes for this work.

References

1 A. J. Appleby and F. R. Foulkes, *Fuel Cell Handbook*, Van Nostrand Reinhold, New York, 1989.
2 S. Srinivasan, *J. Electrochem. Soc., 136* (1989) 41C.
3 K. Prater, in D. G. Lovering (ed.), *Fuel Cells — Grove Anniversary Symposium: 1989*, Elsevier London, 1990, p. 239.
4 E. A. Ticianelli, C. R. Derouin and S. Srinivasan, *J. Electroanal. Chem., 251* (1988) 275.
5 S. Srinivasan, D. J. Manko, H. Koch, M. A. Enayetullah and A. J. Appleby, *J. Power Sources, 29* (1990) 367.
6 I. D. Raistrick, *U.S. Patent 4 876 115* (Oct. 24, 1989).
7 S. Srinivasan, E. A. Ticianelli, C. R. Derouin and A. Redondo, *J. Power Sources, 22* (1988) 359.
8 A. Parthasarathy, C. R. Martin and S. Srinivasan, *J. Electrochem. Soc., 138* (1991) 916.
9 W. Paik, T. E. Springer and S. Srinivasan, *J. Electrochem. Soc., 136* (1989) 644.
10 A. Parthasarathy, B. Dave, S. Srinivasan, A. J. Appleby and C. R. Martin, *J. Electroanal. Chem.*, submitted for publication.
11 A. Parthasarathy, S. Srinivasan, A. J. Appleby and C. R. Martin, paper in preparation.
12 C. P. Winlove, K. H. Parker and R.K.C. Oxenham, *J. Electroanal. Chem., 170* (1984) 293.
13 H. Koch, A. Nandi, N. K. Anand, O. Velev, D. H. Swan, S. Srinivasan and A. J. Appleby, *Ext. Abstr., 178th Meet. of the Electrochemical Society, Seattle, WA, Oct. 14–19, 1990*, Abstr. no. 115.

14 A. Damjanovic and V. Brusic, *Electrochim. Acta, 12* (1967) 615.
15 J. O'M. Bockris and S. Srinivasan, *Fuel Cells: Their Electrochemistry*, McGraw-Hill, New York, 1969.
16 D. A. Landsman and F. J. Luczak, *U.S. Patent 4 316 944* (Feb. 23, 1982); *U.S. Patent 4 373 014* (Feb. 8, 1983).
17 K. Kunimatsu, *Ber. Bunsenges Phys. Chem., 94* (1990) 1025.